
This is an electronic reprint of the original article.
This reprint may differ from the original in pagination and typographic detail.

Ojala, Teemu; Ahmed, Hassan; Kuusela, Petri; Seppänen, Aku; Punkki, Jouni
Monitoring of concrete segregation using AC impedance spectroscopy

Published in:
Construction and Building Materials

DOI:
[10.1016/j.conbuildmat.2023.131453](https://doi.org/10.1016/j.conbuildmat.2023.131453)

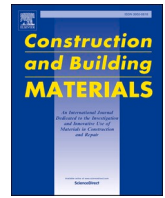
Published: 27/06/2023

Document Version
Publisher's PDF, also known as Version of record

Published under the following license:
CC BY

Please cite the original version:
Ojala, T., Ahmed, H., Kuusela, P., Seppänen, A., & Punkki, J. (2023). Monitoring of concrete segregation using AC impedance spectroscopy. *Construction and Building Materials*, 384, Article 131453.
<https://doi.org/10.1016/j.conbuildmat.2023.131453>

This material is protected by copyright and other intellectual property rights, and duplication or sale of all or part of any of the repository collections is not permitted, except that material may be duplicated by you for your research use or educational purposes in electronic or print form. You must obtain permission for any other use. Electronic or print copies may not be offered, whether for sale or otherwise to anyone who is not an authorised user.



Monitoring of concrete segregation using AC impedance spectroscopy

Teemu Ojala^{a,*}, Hassan Ahmed^a, Petri Kuusela^b, Aku Seppänen^b, Jouni Punkki^a

^a Aalto University, Department of Civil Engineering, Espoo 02150, Finland

^b University of Eastern Finland, Department of Applied Physics, Kuopio 70210, Finland

ARTICLE INFO

Keywords:

Concrete compaction
Vibration time
Segregation
Impedance spectroscopy

ABSTRACT

Segregation is one of the major phenomena decreasing the durability of concrete and increasing its risk of failure. This paper investigates the feasibility of AC Impedance Spectroscopy (ACIS) to serve as a monitoring technique for the concrete segregation during compaction. The impedances of fresh concrete were determined between compaction intervals. Changes in the calculated bulk resistivities were compared to hardened densities of the drilled cores, as well as to aggregate segregation obtained via digital image analysis of the hardened concrete sections. During the compaction process, a significant difference in the bulk resistivity was observed between the top and bottom parts of segregated specimens in comparison to unsegregated specimens. By inspecting the relationship between the measurement methods, it was found that ACIS provides a reliable approach ($r = -0.948$) for estimating the segregation level in cases where the resistivity is mostly affected by the movement of aggregates.

1. Introduction

Normally Vibrated Concrete (NVC) is a widely used building material because of its low-cost, high-strength, and durability. To ensure that NVC reaches its design strength and durability, it must be compacted in its fresh state. Proper compaction of NVC increases its density by packing the aggregates and releasing the entrapped air [1]. However, NVC is at a great risk of segregation during the compaction process [2–4]. Segregation is defined as the separation of concrete constituents due to excessive vibration, which causes inhomogeneity in the hardened concrete [1], several durability complications, and large decreases in strengths [4]. Hence, segregation of NVC should be minimized by tracking the separation of aggregates at the time of compaction.

The behaviour of fresh NVC during compaction largely depends on its workability [1] and rheological properties [5], which are influenced by changes in different ingredients, such as the water content, amount of superplasticizer, and size of aggregates [1]. Adjusting one or more of those constituents might produce concretes with similar slump values but different workability properties, and those concretes will behave dissimilarly when compacted [6]. Therefore, a measurement technique is needed to enable monitoring segregation during the vibration of different NVC mixtures.

Several methods have been developed to assess the segregation of both Self-Compacting Concretes (SCC) [7–11] and Light-Weight

Aggregate Concretes (LWAC) [12–14]. To assess the segregation of LWAC, Ke et al. [12] proposed a segregation index based on the ratio between densities of the top and bottom parts of a LWAC cylinder. On the other hand, Barbosa et al. [14] quantified the ratio of aggregates in photographs of cut sections from hardened LWAC. Similarly, Solak et al. [13] provided segregation indices from digitally treated images of LWAC sections. Analysis of the results in the works by Solak et al. [13] and Barbosa et al. [14] is based on the existence of a correlation between the volumetric fraction of aggregates in a concrete sample and the aggregates detected through image analysis on a section from the same sample. Furthermore, Mouton (2002) as mentioned in Solak et al. [13] showed the proportionality between the area of an object when intersected by arbitrary surfaces and the object's 3D volume in the same reference space. However, all the above methods detect segregation in already hardened concrete, which limits their potential to quality monitoring of already existing structures.

To evaluate the segregation of SCC, Shen et al. [8] designed a segregation probe that measures the thickness of cement paste on top of segregated SCC. Furthermore, Gökçe and Andiç-Çakır [10] created a 3-compartment sieve apparatus that provides the distribution of coarse aggregates in SCC through wet sieving. Additionally, an electrical current method has been used to evaluate various effects of water migration, compaction, and segregation on cementitious materials [15–18]. Furthermore, electrical conductivity measurements were used to

* Corresponding author.

E-mail address: teemu.ojala@aalto.fi (T. Ojala).

<https://doi.org/10.1016/j.conbuildmat.2023.131453>

Received 9 August 2022; Received in revised form 9 March 2023; Accepted 13 April 2023

Available online 21 April 2023

0950-0618/© 2023 The Authors. Published by Elsevier Ltd. This is an open access article under the CC BY license (<http://creativecommons.org/licenses/by/4.0/>).

investigate the segregation of SCC [7,9,11]. Mesbah et al. [7] devised an electrode system to detect the static stability of SCC by measuring the variance of the ionic concentration along a sample. They [7] proposed conductivity-based indices that correlate to the aggregate distributions obtained via wet sieving. Similarly, Nili et al. [9] used electrical resistivity measurements to evaluate the static segregation of SCC with added fly ash and silica fume. A relationship was observed between the mass of coarse aggregates obtained by wet sieving and the resistivity differences. Most recently, Yim et al. [11] developed another electrode system to evaluate the segregation of SCC mixtures with different superplasticizer doses. A significant difference of the electrical resistivity was detected between the top and bottom layers of the segregated samples, which was confirmed by wet sieving.

All the mentioned works investigated techniques for monitoring segregation of SCC. In comparison with NVC, the mix design of SCC contains higher amounts of mineral fillers and larger doses of high-range water-reducing admixtures. For this reason, SCC behaves differently from NVC; most importantly, its segregation differs from NVC segregation, where the latter is usually caused by over-vibration [19]. No studies have been devoted to assessing segregation during the compaction of fresh NVC.

To investigate the properties of cementitious materials, an electronic technique called AC Impedance Spectroscopy (ACIS) has been applied on various experiments as reviewed by Hu et al. [20] and Wang et al. [21]. After McCarter et al. [22] utilised impedance spectroscopy over a wide frequency range of 20 Hz to 110 MHz on the hydrating cement paste, the ACIS has progressively become more promising non-destructive measurement technique; for a recent review, see [21]. In the ACIS analysis of cement based materials, the impedance measurements are often drawn in the form of a Nyquist plot, from which the bulk (ionic) resistance, in Ohms (Ω), is estimated by locating the abscissa of the intersection of the bulk (high-frequency section) and electrode arcs (low-frequency section) [22–26].

To determine the effect of concrete phases with electrical measurements, Princigallo et al. [27] studied the relationship between conductivity, compressive strength and aggregate amount. The researchers found out that the loss in electrical conductivity was highly correlated with the induction period. The presence of aggregates postponed the loss in conductance within the first two hours. Moreover, it was derived that aggregate volume could be estimated from the fresh concrete using a power law equation if the mix dependent parameters are known. A more recent paper by Hou et al. [28] focused on investigating how coarse aggregates affect the resistivity of hardened concrete. They found out that bulk resistivity of concrete is greatly affected by volume of coarse aggregates. Additionally, properties of the coarse aggregates had minor impact on the results.

In contrast to hardened concrete, few recent studies have investigated cementitious materials in their fresh state. McCarter [29,30] determined the complex impedance using Nyquist plots before the setting of Ordinary Portland Cement concrete. Based on his studies, a bulk arc develops rapidly and is strongly related to the volume fraction of aggregates of the concrete, whereas the bulk arc has not been observed in the fresh cement paste. McCarter [30] notes that the addition of the low-conductive aggregates increases the bulk resistance as the time constant of the system transforms into an observable frequency range. More recently, Park et al. [31] estimated the water-to-cement (w/c) ratio by combining the Electrochemical Impedance Spectroscopy (EIS) measurements and machine learning model that predicts w/c ratio of the cement paste. Because of the lack of aggregates, the measurements did not generate the bulk arc as previously also noted by McCarter [30]. Zhu et al. [32] studied the effects of a High-Range Water Reducer during the setting time of the cement paste using EIS. They observed that fluidity, measured by the mini cone test, is related to the charge transfer resistance, computed from the Nyquist curves. These previous findings on hardened and fresh concrete demonstrate the potential of ACIS system in the quality control.

The main objective of this study is to investigate whether ACIS could serve as an online technique to monitor the segregation of NVC during the compaction process—and to provide information for timely decision of stopping the vibration before the segregation occurs. For this purpose, we set up an experiment where ACIS measurements are collected from concrete specimens at different depths and in various stages of compaction. The results of ACIS are corroborated with two indices derived from the analysis of hardened specimens: density measurements of drilled cores at different depths and digital image analysis based aggregate ratios at different depths.

2. Materials and methods

2.1. Materials

The concretes were proportioned using Sulphate-Resistant (SR) cement CEM I 42.5 N, manufactured by Finnsementti (Parainen, Finland). SR-cement was chosen to promote segregation based on the preliminary tests and lower Blaine fineness of 310–390 m²/kg. The chemical composition of the SR cement is presented in Table 1.

All the aggregates were granitic gravel that were washed, dried, and graded by sieving before the experiment. A total of seven different aggregate fraction sizes were combined, for which the maximum aggregate size was 16 mm. The aggregate size distribution and mix composition are shown in Table 2. The specific gravities of the cement and aggregates were 3.15 and 2.68, respectively. The filler was also graded by sieving before making the mix composition. The mix composition included 400 kg/m³ of SR cement, 160 kg/m³ of effective water and 1755 kg/m³ of aggregates. The water absorption of all the fractions was 0.8%, leading to an effective w/c ratio of 0.40. In addition, the concrete was air-entrained using MastersBuilders MasterAir 100 (Riihimäki, Finland) with a dosage of 0.032% by the weight of cement, and superplasticised using MasterBuilders MasterGlenium SKY 600 (Riihimäki, Finland) with a dosage of 0.9% by the weight of cement. All the components were stored and used at room temperature (20 ± 2 °C) in laboratory conditions. For each experiment, a 30-litre batch of concrete was prepared in a pan-type mixer (Pemat ZZ 75 HE).

2.2. Standard tests and density measurements

Two fresh concrete tests were performed after initial mixing of the concrete. The consistency was evaluated through the slump test EN 12350-2:2019 and air content through pressure method test EN 12350-7:2019. To achieve comparable mixtures, the target slump was set to 250 mm where actual values varied between 245 and 255 mm, and the target air content was set to 6.0% where actual values varied between 5.9 and 6.7%. If the mixture did not meet the target slump and/or air content, the mixture was discarded, and a new concrete mixture was batched until both properties were met.

For the hardened concrete tests, three 75-mm cores were drilled from the top, middle and bottom parts of each specimen, as shown in Fig. 1. The densities of the cores were determined according to the standard EN 12390-7:2019. In addition, vertical sections were sawn from the electrode side of each specimen with a thickness of 20 ± 2 mm, which were prepared for the Digital Image Analysis (DIA).

Table 1

The chemical composition of the Sulphate-Resistant (SR) cement CEM I 42.5 N.

Chemical composition	Mass percentage volume (%)
CaO	64–66
SiO ₂	20–22
Al ₂ O ₃	3.1–3.7
Fe ₂ O ₃	3.9–4.2
MgO	2.7–3.5
Limestone	≤5

Table 2
Combined aggregate size composition and distribution of the mixture.

Aggregate type	Fraction (Diameter in mm)	Portion (%)	Sieve size (mm)										
			0.125	0.25	0.5	1.0	2.0	4.0	8.0	16.0	32.0	64.0	
Filler	Filler 96	8	42	81	93	97	98	100	100	100	100	100	100
Fine Aggregates (FA)	0.1 – 0.6	12	3	21	76	100	100	100	100	100	100	100	100
	0.5 – 1.2	12	0	2	6	70	100	100	100	100	100	100	100
	1.0 – 2.0	15	0	1	2	7	79	100	100	100	100	100	100
	2.0 – 5.0	15	0	0	1	1	1	47	100	100	100	100	100
Coarse Aggregates (CA)	5.0 – 10.0	18	0	0	0	0	0	3	82	100	100	100	100
	8.0 – 16.0	20	0	0	0	0	0	0	5	99	100	100	100
	Total (%)	100											
	Combined Aggregates (%)		4	9	18	29	44	55	78	100	100	100	100

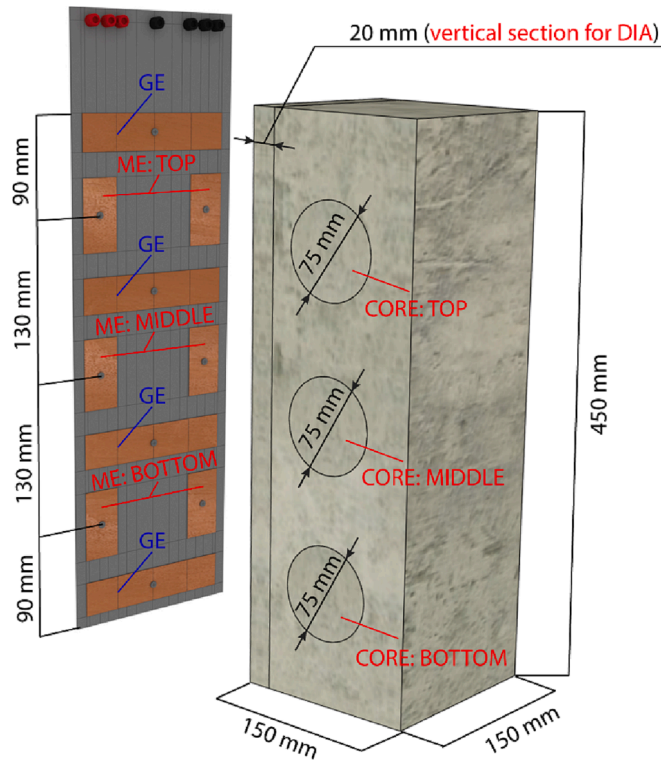


Fig. 1. An illustration of the fabricated electrode panel that consists of three Measuring Electrodes (ME) layers (top, middle, and bottom), Grounding Electrodes (GE) and the locations of the drilled cores (top, middle, bottom) and the vertical section in the specimen.

2.3. Digital Image Analysis (DIA)

DIA was carried out in three steps to digitally estimate the ratio of coarse aggregates in each specimen as presented in Fig. 2. The following procedure was performed on the seven 20-mm vertical sections that were sawn from the electrode side of each specimen. In the first step, the sections were photographed using a digital SLR camera, which was placed perpendicularly towards the surface. To enhance the visual contrast of the sawn sections, their surfaces were wetted with a moist sponge just before capturing the images. Due to the large surface area of the section, two images were captured from the top and bottom and combined in Adobe Photoshop into a single image that has a total spatial resolution of 9000 × 3000 px² after resizing. In the second step, the larger aggregates were manually selected in Adobe Photoshop, and the result was saved as a binary image for further processing. In the third step, aggregates with an equivalent diameter smaller than 8.0 mm were removed, and the ratio of the coarse aggregates was calculated automatically using a Matlab script. For the analysis, three Regions of

Interest (ROI), having an area of 150 × 100 mm, were selected based on the layout of the electrodes and the locations of the drilled cores. Based on the calculated pixel density of 20.0 px/mm, the top, middle, and bottom ROIs corresponded to the pixel rows 1000–3000, 3600–5600, 6200–8200 in the digital images, respectively. The Ratio of the Coarse Aggregates (RCA) was calculated by ratio of white pixels in the binary mask in each ROI.

2.4. AC impedance spectroscopy measurements and data analysis

The specimens were cast into a special mould (510 × 150 × 100 mm³) that was made of non-conducting polyvinyl chloride (PVC). A specially fabricated electrode panel (Fig. 1) was attached into the mould, consisting of a backing PVC plate, electrodes, and coaxial cables leading to the connectors on top of the panel. The shells of the coaxial cables were grounded for interference protection. The electrodes were cut from a thin copper sheet and glued on the PVC plate using an epoxy adhesive then fixed using bolts and nuts. Measuring Electrodes (MEs) were installed in three measurement layers: top, middle, and bottom, where each ME had the dimensions of 60 × 30 mm² (Height × Width). Grounding Electrodes (GEs) were installed between the MEs to reduce the effect of the electric field spreading to other measurement layers. In addition, a grounding back plate was glued between the panel and the wires, covering the whole section of the panel inside the mould. The wires were connected to seven banana plugs, six of which were connected to the MEs and one to the ground. A schematic diagram is presented in Fig. 3 that shows the electrodes and wire configuration of the panel.

Fig. 4 shows the monitoring system, which consists of an impedance analyser (Hioki 3532–50 LCR HiTester), a laptop (SpecAn operating software), and the mould with the attached electrode panel. To compact the concrete, the mould was fixed on the surface of a vibrating table with adjustable frequencies and a timer switch. During the compaction, the impedance analyser was connected to the electrode panel with two coaxial cables through banana plugs. To switch measurements from one layer to another, the two coaxial cables were physically moved among the banana plugs to connect to each pair of MEs associated with the desired layer.

AC impedance measurements were used because DC resistance measurements are affected not only by the resistance of concrete but also by the contact impedances between electrodes and concrete. With DC, the impedance is very high because of the so-called polarization effect on the electrode-concrete interface. The use of AC current both reduces the polarization effect and enables distinguishing between the impedances of concrete and the electrode-concrete interface.

The electrical impedance can be written in the following forms

$$Z(\omega) = |Z(\omega)| \bullet e^{j \bullet \text{Arg}(Z(\omega))} = \text{Re}(Z(\omega)) + j \bullet \text{Im}(Z(\omega)) \tag{1}$$

where $Z(\omega)$ is the electrical impedance, $|Z(\omega)|$, $\text{Arg}(Z(\omega))$, $\text{Re}(Z(\omega))$ and $\text{Im}(Z(\omega))$ are its magnitude, argument, real part, and imaginary part (reactance), respectively, and ω is the angular frequency of the alter-

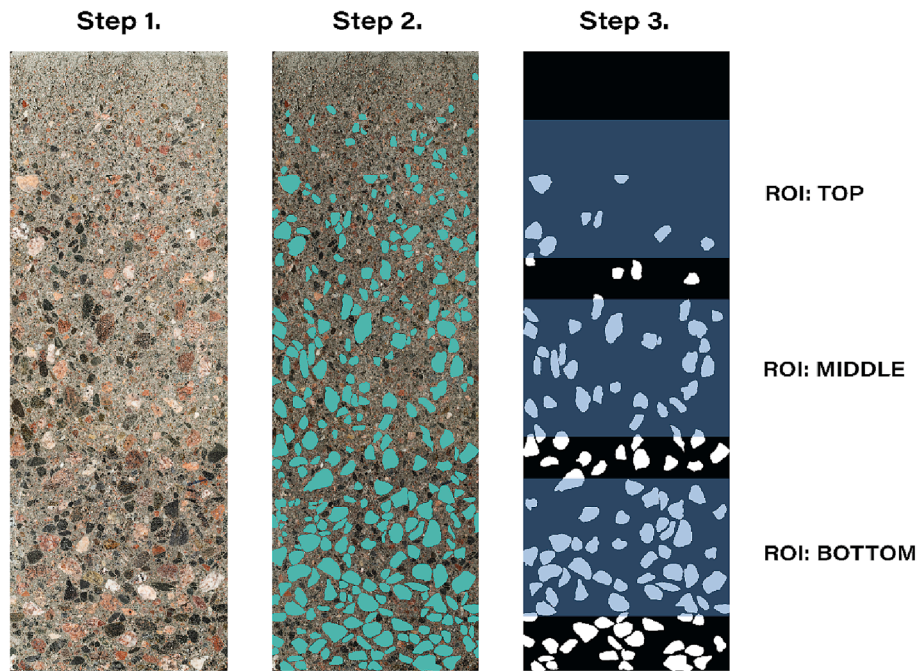


Fig. 2. Three steps in the Digital Image Analysis which were: 1) A combined image of two photographs, 2) Manually masked image, 3) Filtered binary image with visualised Region of Interests (ROIs) of top, middle, bottom locations.

nating current. The frequency dependent impedance is determined by sinusoidal voltage excitations and current measurements, or vice versa, from which the impedance is determined

$$Z(\omega) = \frac{V(\omega)}{I(\omega)} = \frac{|V(\omega)|}{|I(\omega)|} \bullet e^{j\varphi(\omega)} \quad (2)$$

where $|V(\omega)|$ and $|I(\omega)|$ are the amplitudes of the sinusoidal voltage and current, respectively, and $\varphi(\omega)$ is the phase shift between the voltage and current. Eqs. (1) and (2) imply that $|Z(\omega)| = |V(\omega)|/|I(\omega)|$ and $\text{Arg}(Z(\omega)) = \varphi(\omega)$.

Impedance measurements were collected using voltage excitations of amplitude $|V(\omega)| = 1$ V, and a set of seventeen frequencies: $f = \omega/2\pi = 42$ Hz, 50 Hz, 75 Hz, 100 Hz, 500 Hz, 1 kHz, 6 kHz, 12 kHz, 25 kHz, 37 kHz, 74 kHz, 123 kHz, 185 kHz, 200 kHz, 500 kHz, 1 MHz, and 2 MHz. Before the experiments, the calibration of the impedance analyser was executed to avoid the effects of non-ideal short or open circuit impedance measurements. This was done via the calibration options in the device settings.

Determination of the bulk resistance (R_b) of the concrete material based on the so-called Nyquist plot is illustrated by an example in Fig. 5. The Nyquist plot represents $-Im(Z(\omega))$ vs. $Re(Z(\omega))$ at different frequencies, and R_b can be determined as the abscissa of the intersection of bulk and electrode arcs [22–26]. In Fig. 5, the Nyquist plots representing the impedances at three electrode layers (top, middle and bottom) are shown.

The three bulk resistances in Fig. 5 differ from each other due to the depth dependence of the concrete composition. However, the three resistances are also affected by the geometry of each electrode layer, especially because in this electrode setup, the electric current is spread in the entire volume of the concrete material – thus partly also outside the layer where the excited electrodes are – and for this reason, the volumes that affect measurements at different depths differ in their geometries. To reduce the effects of geometry differences (and other modelling errors such as variations in the electrode contacts) on the ACIS based segregation index, the bulk resistance of the concrete was transformed into a bulk resistivity (BR) of the concrete. To compute the required geometric constants for each layer (top, middle, bottom), a

water resistivity (ρ) of $52 \Omega \cdot m$ was measured from the tap water in the laboratory. Thus, geometric constants for each layer were calculated using the equation

$$k_i = \frac{R_{b_i}(\text{water})}{\rho} \quad (3)$$

where k_i is the geometric constant [m^{-1}] for each layer $i = 1, 2$ and 3 , $R_{b_i}(\text{water})$ is the bulk resistance of the water, and ρ is the water resistivity of $52 \Omega \cdot m$. The given equation yielded geometric constants of $101.3 m^{-1}$, $118.1 m^{-1}$, and $108.5 m^{-1}$ for the top, middle, and bottom layers, respectively. Afterwards, the concrete bulk resistivities were calculated using the equation

$$BR = \frac{R_{b_i}(\text{concrete})}{k_i} \quad (4)$$

where BR is the bulk resistivity of concrete [$\Omega \cdot m$], $R_{b_i}(\text{concrete})$ is the bulk resistance of concrete [Ω], k_i is the geometric constant [m^{-1}] for each layer $i = 1, 2, 3$. Finally, the calculated BR of each concrete layer was used in the ACIS analysis.

2.5. Compaction experiment for testing AC impedance spectroscopy

A total of seven concrete specimens were cast and compacted. For each specimen, the mould was fixed on the vibrating table and filled in one-layer with concrete. As shown in Table 3, the specimens were labelled as S130-1, S130-2, S130-3, S130-4, S90-1, S90-2, and S50-1, and were divided into three categories based on the total vibration time. The first four specimens were vibrated for 130 s, while the following two were vibrated for 90 s, and the last one was vibrated for 50 s. These vibration times were tested to cause low to high segregation in the experimented high fluidity concrete. The ACIS measurements were taken between the vibration time steps shown in Table 3. The vibrating table was connected to power source throughout the experiment. The vibration frequency of the table was set to 86 Hz for the first 50 s of vibration for all the groups. Afterwards, the vibration frequency was increased to 129 Hz for the first two groups to further enhance the possibility of segregation to occur. The whole procedure, for a total

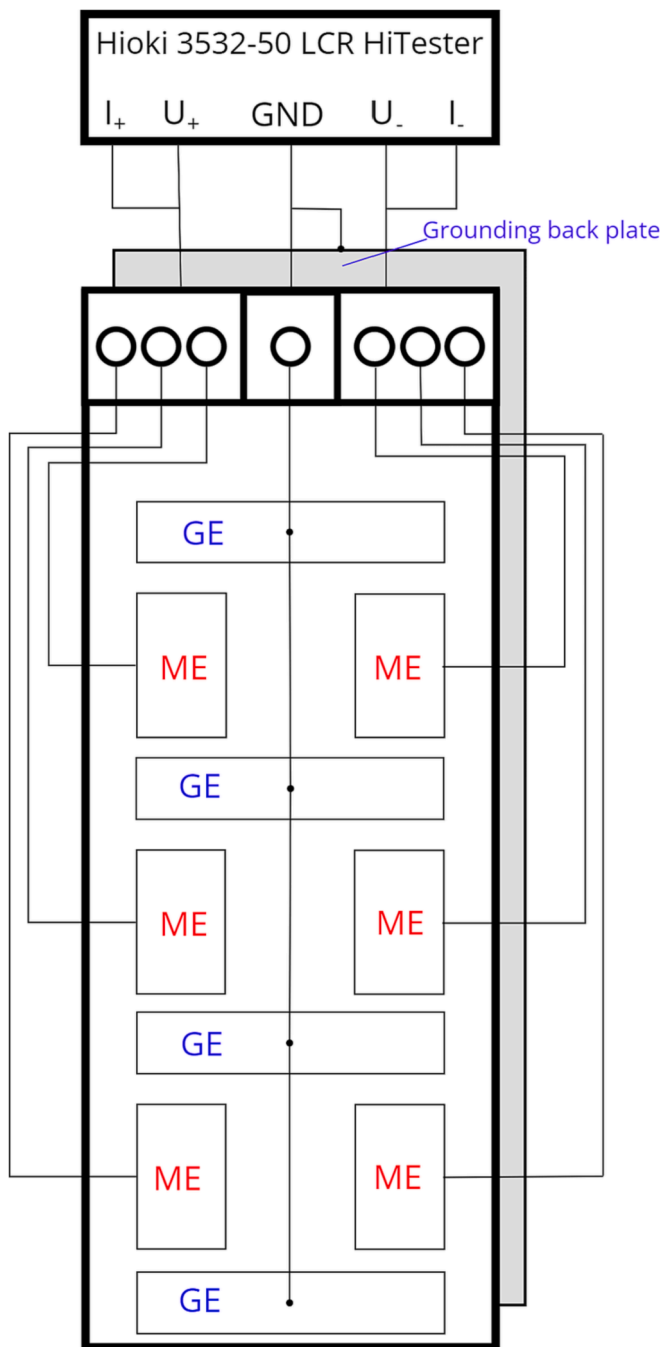


Fig. 3. The schematic diagram of the electrodes and wire configuration.

vibration time of 130 s, took 80 min as the frequency sweep for each layer lasted approximately 6 mins, during which the concrete stayed in the fresh state.

3. Results and discussion

3.1. Results of AC impedance spectroscopy

Fig. 6 shows the BR values as a function of time for the top, middle, and bottom layers of specimens S130-1 and S90-2. In the context of the following analysis, concrete consists of three phases: cement paste, aggregates, and compaction pores, where cement paste is electrically conductive and the other two are electrically insulating. The electrical insulation is due to the fact that both aggregates and compaction pores

fill the space of the cement paste resulting in currents taking longer paths between the electrodes and increasing the BR.

Firstly, as shown in Fig. 6a, the BR of the top layer of S130-1 rose steadily until 50 s. This steady increase can be caused by the rise of compaction air into the top layer from the middle layer. This was followed by a sharper increase in BR until 90 s, which might be a result of the accumulation of air from both the middle and the bottom layers. The BR of the top layer plummeted after 90 s, which can denote the occurrence of segregation, as aggregates sink out of the top layer while compaction air escapes. As a result, the top layer contained more cement paste than the other two phases, hence the plummet in BR.

Secondly, the BR of the middle layer of S130-1 slightly fluctuated with an overall small increase until 70 s of vibration. This fluctuation can be caused by the fact that during that time the loss of compaction air to the top layer was compensated for by gaining air from the bottom layer. Similarly, aggregates were both sinking towards the middle layer from the top, while some aggregates were sinking from the middle layer to the bottom. After 70 s of vibration, there was a more pronounced decrease in BR, which might be caused by a larger net loss of aggregates that sunk to the bottom layer.

Lastly, for S130-1, the BR of the bottom layer showed small variations during the first 70 s, with an overall trend of a slight decrease, which was caused by the escapement of compaction air, and followed by a very sharp increase in BR. That sharp increase can be justified by the accumulation of aggregates from the upper layers, which is supported by the decrease in BR for both the top and middle layers.

On the other hand, for S90-2 (Fig. 6b), the BR of the top layer constantly decreased after a minor increase during the first 10 s, which is the opposite of what happened in the top layer of S130-1. This difference can be caused by the fact that, in S90-2, aggregates were sinking from the top layer at a higher rate –and in larger amounts– than that of S130-1, which can be confirmed by later inspections of the amount of aggregates in each of the top layers. However, a similar plummet in the BR of the top layer occurred at 50 s.

As for the middle and bottom layers of S90-2, they both followed very similar trends to their counterparts of S130-1, where the BR of the middle layer significantly decreased and that of the bottom layer sharply rose at 50 s. Hence, it is believed that S90-2 was also segregated.

As discussed above, the top and middle layers show similar development of resistivity over the vibration time, while the bottom layer behaves in the opposite manner, which indicates the occurrence of segregation. To investigate the segregation in the seven specimens, the differences between BR of the top and bottom layers are plotted in Fig. 7. For all the specimens, small fluctuations in the difference of BR occurred during the first 50 s of vibration. These small fluctuations indicate either minor changes in the three phases of concrete between the top and bottom layers, or that those changes were cancelled out, as the removal of aggregates can be followed by an increase of air in the top layer or the opposite in the bottom layer.

As the vibration time exceeds 50 s, the difference in BR between the top and bottom layers increases significantly for all the specimens, except for S90-1, which shows a smaller change. Those larger differences can be associated with higher levels of segregation as explained previously, while S90-1 might have not segregated as much. Those five specimens with higher differences in BR can be categorized into two groups: one that displays a sharp increase in the difference of BR followed by a plummet, and the other follows an overall downward trend. The first group contains specimens S130-1 and S130-2, which, as explained previously, could have had air accumulated at the top layer causing a sharp increase in BR, which was followed by a plummet as the air escapes and the aggregates sink more towards the bottom layer. The second group includes specimens S130-3, S130-4, and S90-2, for which the aggregates could have sunk much quicker or with higher amounts from the top layer.

Notably, specimens that were vibrated for the same time did not have a similar change over time of the BR difference between their top and

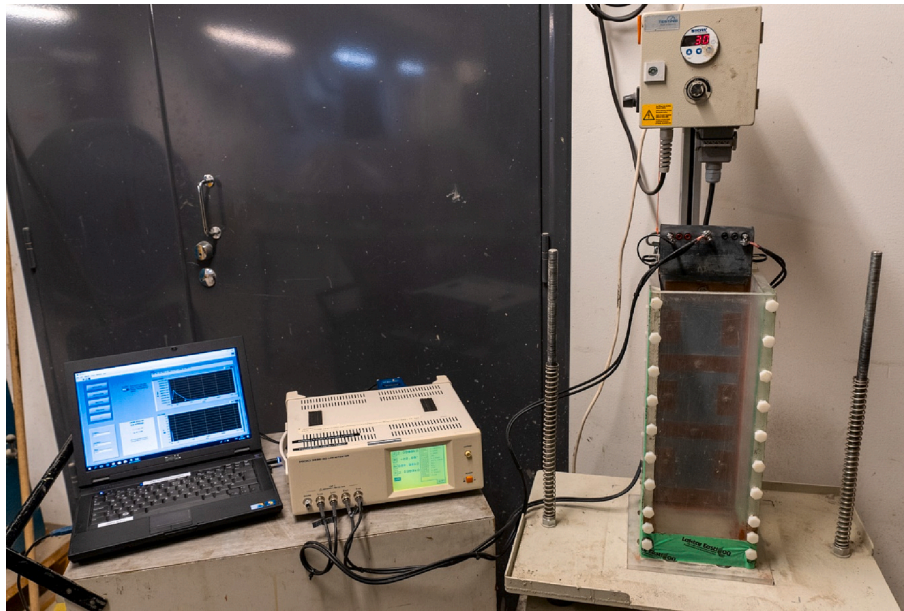


Fig. 4. A photograph representing the experimental setup. The measurement system consists of an impedance analyser, and a laptop with the measurement software. The electrode panel is integrated on the mould which is fixed on the vibrating table.

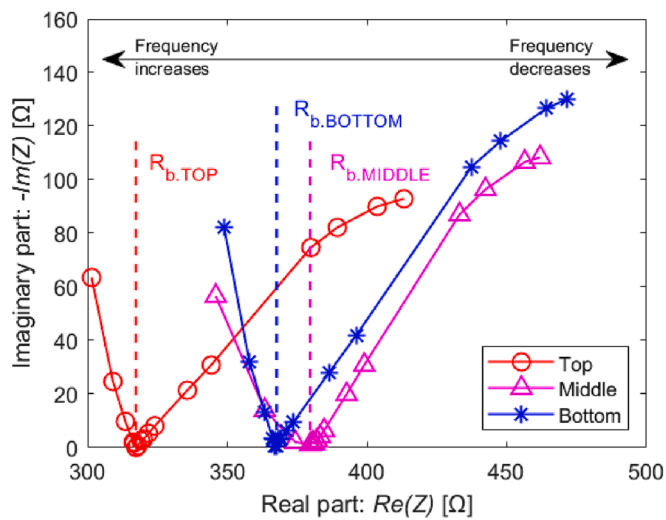


Fig. 5. ACIS measurements, examples of Nyquist plots for fresh concrete; the frequency range is 42 Hz – 2 MHz. The three plots represent measurements from electrode pairs at three different depths.

Table 3

Classification of concretes, vibration time, number of tested specimens, and codenames used in the analysis.

Specimen	S130-1 S130-2, S130-3, S130-4	S90-1 S90-2	S50-1
Total vibration time (s)	130	90	50
Time steps (s) using vibrational frequency of 86 Hz	10, 20, 30, 40, and 50	10, 20, 30, 40, and 50	10, 20, 30, 40, and 50
Time steps (s) using vibrational frequency of 129 Hz	70, 90, and 130	70, 80, and 90	None

bottom layers, and their final BR differences were quite varied. This supports the need for an objective method to monitor segregation during compaction. Hence, the authors propose the following segregation index

for BR difference, SI_{BR} , which defines the segregation based on the differences of BR between the top and middle layers at the final vibration time:

$$SI_{BR} = BR_{final(top)} - BR_{final(bottom)} \quad (5)$$

where SI_{BR} is the BR segregation index [$\Omega \cdot m$], $BR_{final(top)}$ is the final BR in top layer [$\Omega \cdot m$], and $BR_{final(bottom)}$ is the final BR in bottom layer [$\Omega \cdot m$].

3.2. Results of DIA versus AC impedance spectroscopy

Table 4 shows the Ratios of the Coarse Aggregates (RCA) that was estimated based on the DIA method, as well as the differences in RCA between the top and bottom layers. These differences in aggregate content for each specimen can be presented using the following equation

$$SI_{RCA} = RCA(top) - RCA(bottom). \quad (6)$$

where SI_{RCA} is the aggregate segregation index in percentage points [pp], $RCA(top)$ is the RCA of the top layer [%], and $RCA(bottom)$ is the RCA of the bottom layer [%].

Specimens S130-4, S90-2, S130-3 have high segregation indices by aggregates: $SI_{RCA} = 24$ pp, $SI_{RCA} = 23$ pp, $SI_{RCA} = 19$ pp, respectively. These high indices correspond to a high level of segregation due to the sinking of aggregates towards the bottom of the concrete. On the other hand, the values of SI_{RCA} for the remaining four specimens range from 7 pp to 11 pp, which corresponds to a low level of segregation.

To investigate the relationship between the ACIS measurements and the segregation of aggregates in concrete, the SI_{RCA} are plotted against the SI_{BR} for the seven specimens in Fig. 8. A very strong correlation of $r(5) = -0,948$ and $p < 0.012$ (significance level of $\alpha = 0.05$) was found between the two indices, which suggests that the ACIS measurements can estimate the RCA in the compacted concrete. The authors note that linear regression is used in this paper only to quantify the correlation between the RCA and the BR. This does not mean that the dependence of the BR on the aggregate ratio is linear. In contrast, the aggregates affect the paths of the electric current in the material in a complex manner, as pointed out by Hou et al. [28].

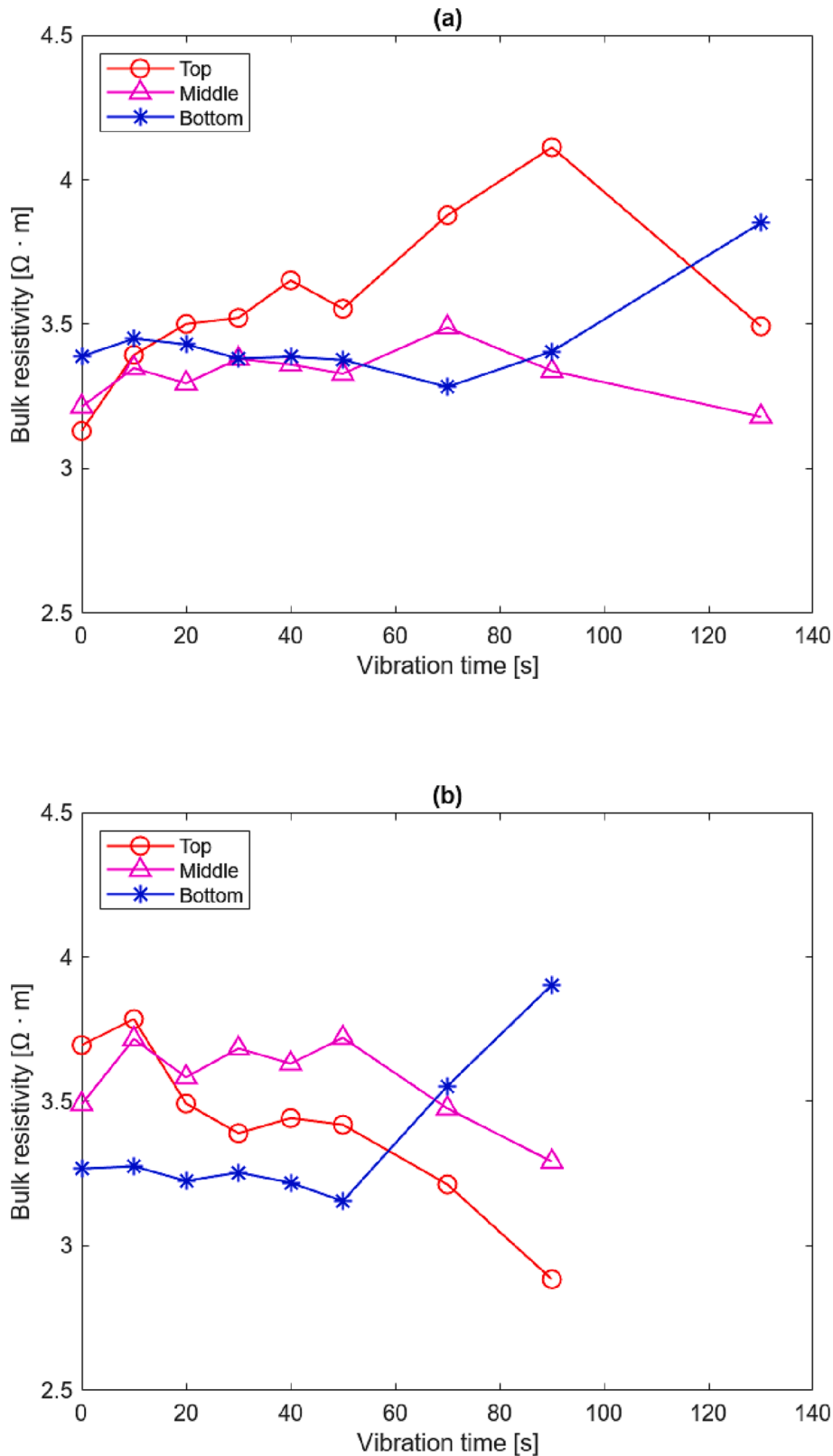


Fig. 6. Development of the Bulk resistivities over the vibration time for specimens: (a) S130-1, and (b) S90-2.

3.3. Results of density versus AC impedance spectroscopy

To estimate the segregation of the specimens, based on the densities of the drilled cores, a segregation index for the difference between the densities of the top and bottom cores can be calculated using the

equation

$$SI_{DEN} = Density(top) - Density(bottom) \tag{7}$$

where SI_{DEN} is the aggregate segregation index [kg/m^3], $Density(top)$ is the density top core [%], and $Density(bottom)$ is the density of the bottom

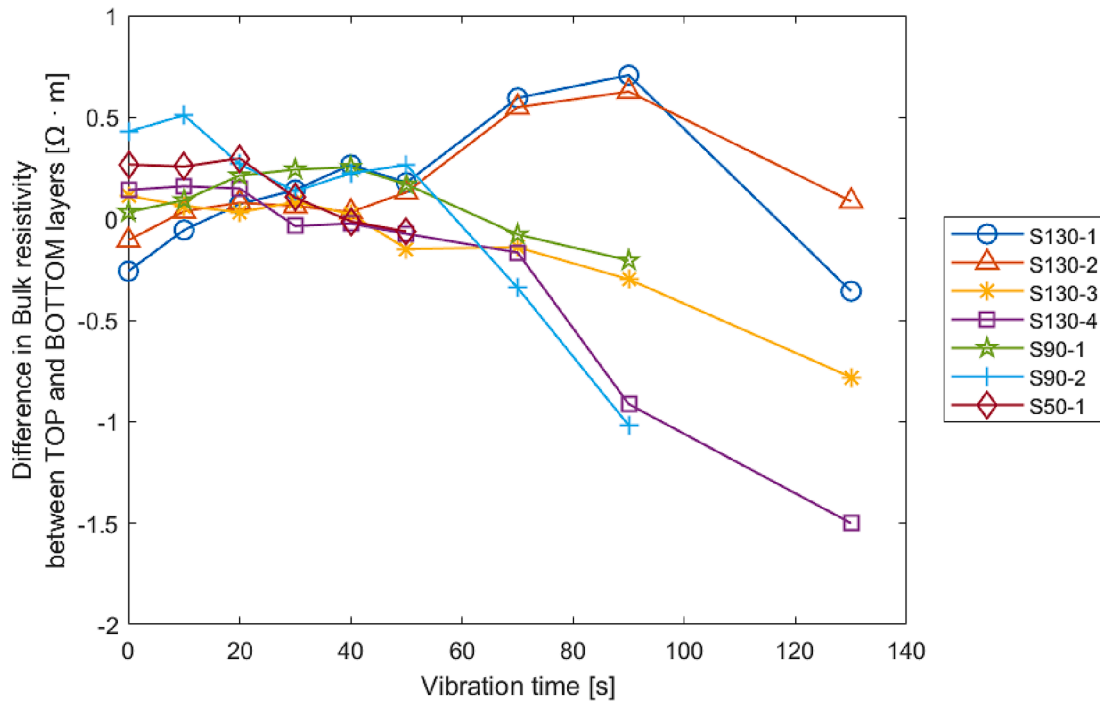


Fig. 7. The difference of the bulk resistivities between the top and bottom part of the specimens as a function of vibration time.

Table 4

The ratios of coarse aggregates (RCA) acquired using DIA and the differences of RCA between the top and bottom values (SI_{RCA}).

	RCA via DIA			SI_{RCA}
	Top	Middle	Bottom	
S130-1	13%	14%	24%	11 pp
S130-2	11%	21%	21%	9 pp
S130-3	6%	17%	26%	19 pp
S130-4	5%	18%	29%	24 pp
S90-1	16%	14%	24 %	8 pp
S90-2	7%	10%	29%	23 pp
S50-1	12%	9%	19%	7 pp

core [%]. The value of SI_{DEN} was over 120 kg/m^3 for specimens S130-1, S130-3, S130-4, and S90-2. These relatively large indices represent the occurrence of severe segregation within the specimens between the top and bottom layers. Similarly, specimens S130-2 and S50-1 had SI_{DEN} values of 73 kg/m^3 and 83 kg/m^3 , respectively. Such values indicate that specimens S130-2 and S50-1 were also segregated but with less severity. The segregation of all above specimens can be caused by aggregates sinking down during the compaction, the concentration of compaction pores towards the top, or a combination of both. On the other hand, S90-1 has the lowest SI_{DEN} of 43 kg/m^3 , which indicates a relatively lower level of segregation compared with the other six specimens. Further, the standard deviation of the density was lowest in specimen S90-1: 21 kg/m^3 . This was 43 kg/m^3 lower than the highest density standard deviation (specimen S130-1), and 9 kg/m^3 lower than that of S130-2, which is the second lowest. This further supports that segregation in S90-1 was much lower than in the rest.

It should be noted that S130-1 was the most segregated according to density measurements with an $SI_{DEN} = 157 \text{ kg/m}^3$, which is more than twice that of S130-2. However, SI_{RCA} of S130-1 and S130-2 are similar: $SI_{RCA} = 11 \text{ pp}$, $SI_{RCA} = 9 \text{ pp}$, respectively. This suggests that the difference in densities in S130-1 was caused by the difference in compaction pores level, and not just the difference in aggregate contents. Furthermore, after inspection of the hardened vertical sections of all specimens, it was noted that the top part of S130-1 had a larger number

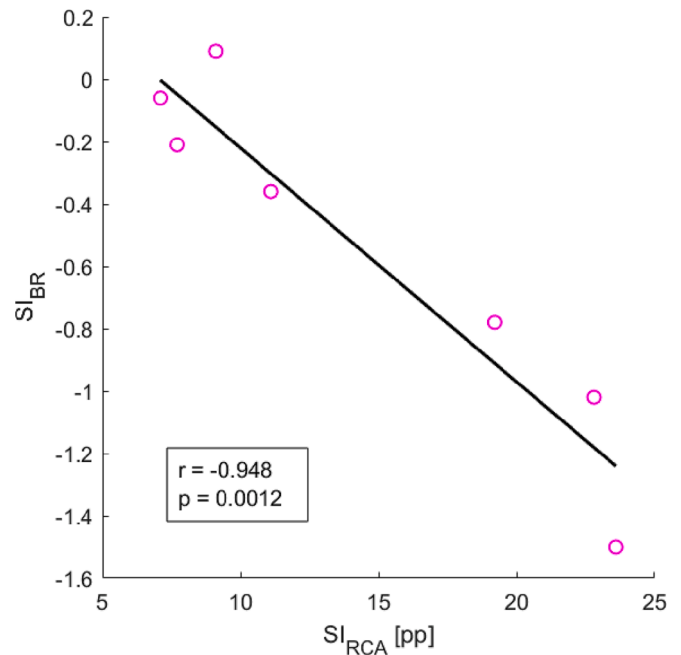


Fig. 8. The relationship between difference in ratio of coarse aggregates (SI_{RCA}) and difference in bulk resistivity (SI_{BR}) measurements for the seven specimens.

of pores when compared with the other sections. This was also reflected in its lower density of 2241 kg/m^3 as shown in Table 5, which was 77 kg/m^3 less than the average of the densities of the other specimens. The reason why SI_{DEN} shows a higher level of segregation than SI_{RCA} for S130-1 can be explained by the fact that SI_{DEN} reflects a combination of the amount of aggregates, air, water, and cement paste in the concrete, while SI_{DEN} takes into account the amount of aggregates only.

The correlation between SI_{BR} and SI_{DEN} is shown in Fig. 9. The two indices show a correlation of $r = -0.703$ with $p = 0.078$, which is much lower than that between SI_{BR} and SI_{RCA} . The much stronger correlation

Table 5

The densities and statistical parameters of the drilled cores in the seven concrete specimens.

	Measured Density [kg/m ³]			Density Statistical Parameters [kg/m ³]	
	Top	Middle	Bottom	Mean	SI _{DEN}
S130-1	2241	2317	2398	2319	157
S130-2	2333	2370	2406	2370	73
S130-3	2321	2377	2462	2387	141
S130-4	2309	2380	2463	2384	154
S90-1	2321	2366	2365	2351	43
S90-2	2315	2355	2443	2371	128
S50-1	2308	2331	2391	2343	83

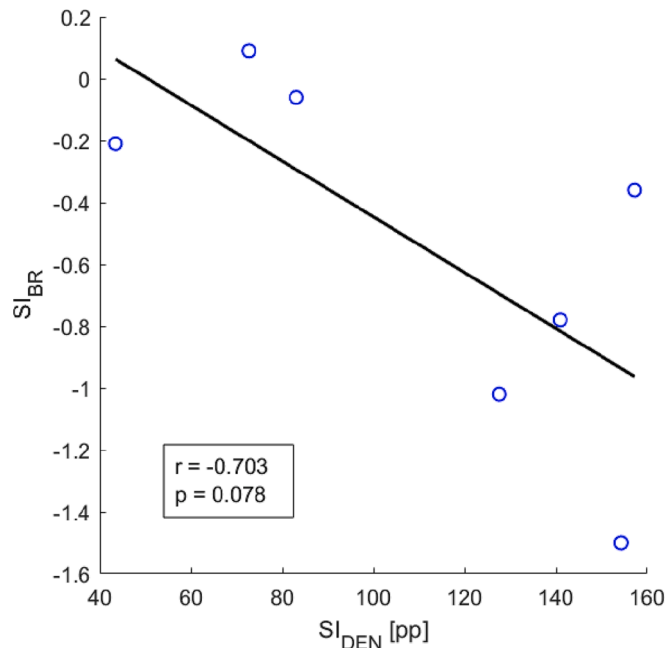


Fig. 9. The relationship between the difference in density of the drilled cores (SI_{DEN}) and difference in the bulk resistivity measurements (SI_{BR}) for the seven specimens.

between ACIS measurements and aggregate ratios could be explained by the fact that the movement of coarse aggregates provides a much more pronounced change in resistivity than that caused by compaction pores in the fresh concrete, i.e., the current is obstructed more strongly as more aggregates accumulate in that location. Conversely, the poorer correlation between SI_{BR} and SI_{DEN} can be explained by the fact that density differences do not only rely on the amount of aggregates as previously described.

As mentioned above, S130-1 had a high amount of air at the top part. This air increases the resistivity of that part, whereas rising of paste and sinking of aggregates tend to decrease the electrical resistivity at the same time. These two opposing effects on resistivity caused the SI_{BR} do to not correlate well with the SI_{DEN} of specimen S130-1, as shown in Fig. 9. Excluding S130-1 from the correlation analysis would significantly strengthen the correlation between SI_{DEN} and SI_{BR}, as it increases the correlation coefficient from -0.703 to 0.873 . However, this exclusion does not affect the correlation between SI_{RCA} and SI_{BR}.

3.4. General discussion

Based on the above results, the level of concrete segregation may dramatically vary among concrete specimens that are vibrated at the same frequency for the same vibration times, even if those specimens are cast from comparable concrete mixtures. This especially shows in the

differences of density and DIA results between the specimens S90-1 and S90-2 where the two segregation indices SI_{DEN} and SI_{RCA} of S90-2 are almost three times those of S90-1. Similarly, although S130-1, S130-2, S130-3, and S130-4 are all vibrated for 130 s, they have a large variation SI_{RCA} among them. These variations in the segregation indices show that the reliance on vibration time is not enough to ensure a high-quality concrete with low segregation. Additionally, it supports the need for developing a method that can monitor the segregation level of fresh concrete during the compaction process.

In this study, the authors investigated the use of ACIS to evaluate segregation in concrete. This method has the advantage of measuring segregation in fresh concrete, unlike density measurements that require the concrete to harden. However, density values were used as a reference for the acquired ACIS measurements. The results showed how the segregation index acquired via density measurements, SI_{DEN}, is unable to distinguish between the decrease in density caused by the lack of aggregates and the drop in density resulting from the presence of air. On the other hand, the reliance on DIA to assess segregation provides a segregation index, SI_{RCA}, which represents segregation solely caused by the movement of aggregates. Based on the results of the experiments, it was found that SI_{BR} has a very strong correlation with SI_{RCA}, which suggests the viability of using ACIS to monitor the process of segregation during compaction.

To the best of the authors knowledge, ACIS was shown to be a promising method to investigate the static segregation of SCC [7,9,11], and based on the results of our study, there are plenty of opportunities for future research related to detecting segregation during the vibration of NVC. The main possibility for further investigation is to test other concrete mixtures with different slump levels and aggregate sizes. Furthermore, testing new concretes will provide more values for the three segregation indices: SI_{DEN}, SI_{RCA}, and SI_{BR}, which will provide a deeper investigation of the correlation between the three. Additionally, the set-up of electrodes could be modified to only include top and bottom layers, since the behaviour of the middle layer was found to be relatively uninfluencing on the results.

It should also be noted that there are some limitations to this study. In the current setup, the ACIS measurements require a long time to complete, which can be improved by replacing the currently used manual switching between electrode layers to an automated switching system and focusing on a smaller frequency range. However, it is worth noting that the more frequencies used, the better the approximation of the bulk resistance. Secondly, the devised electrode panel can only be used in laboratory settings, as it has not been tested for in-situ applications. Lastly, with the present setup, this method cannot monitor segregation in concretes during the vibration by poker vibrators since the material of the vibrator will interfere with the ACIS measurements. However, this can be fixed, for example, by covering the vibrator with electrically insulating material, or by setting vibration time intervals and measuring the impedance in between those intervals when the poker vibrator has been pulled out of the concrete.

4. Conclusions

Conventionally vibrated concrete is susceptible for segregation during compaction. Thus, there is a demand for an online monitoring technique that can be used to control the compaction and to avoid segregation of concrete. In this paper, we investigated experimentally whether an ACIS based monitoring system could provide information on the concrete segregation. For this purpose, we cast a set of specimens and used an integrated electrode panel attached to the mould, to measure electrical resistances of concrete in different depths within the mould at different stages of compaction. Based on the results of this study we draw the following conclusions:

- The ACIS measurements are sensitive to concrete segregation. During the compaction process of the unsegregated specimens, the

difference in the resistivities between top and bottom (SI_{BR}) fluctuates within a much smaller range, when compared to SI_{BR} of the segregated specimens.

- The results given by ACIS are in good agreement with the Digital Image Analysis (DIA): The correlation between the ACIS based index SI_{BR} and the DIA based index SI_{RCA} for the ratio of the coarse aggregates is strong (in this study, the correlation coefficient of -0.948 was determined).
- Measuring the densities from the drilled cores is an inferior method for assessing the level of segregation because of many factors that affect the density of concrete, such as the air content.
- The vibration time does not give a sufficient prediction of the segregation: In the experiments of this study, the segregation level varied dramatically between specimens that were vibrated at the same frequency for the same vibration times, even when those specimens were cast from the same concrete mix recipe until the fresh concrete properties were matched.
- Developing ACIS for the segregation assessment is an attractive alternative because it enables online monitoring: While, e.g., the density measurements from the drill cores are possible only after concrete hardening, the ACIS measurements could be used for determining the segregation level of fresh concrete during the compaction process.
- Further development of the ACIS based testing method is still needed; especially, the electrode setup needs to be designed so that it can be connected to, e.g. a poker vibrator in concrete sites.

Overall, the results of the paper indicate that the ACIS system could serve as a tool for monitoring the segregation of concrete.

CRedit authorship contribution statement

Teemu Ojala: Conceptualization, Formal analysis, Investigation, Writing – original draft, Visualization, Data curation. **Hassan Ahmed:** Formal analysis, Investigation, Writing – original draft, Data curation. **Petri Kuusela:** Methodology, Data curation, Validation. **Aku Seppänen:** Conceptualization, Methodology, Resources, Writing – review & editing, Funding acquisition. **Jouni Punkki:** Resources, Writing – review & editing, Supervision, Funding acquisition.

Declaration of Competing Interest

The authors declare that they have no known competing financial interests or personal relationships that could have appeared to influence the work reported in this paper.

Data availability

Data will be made available on request.

Acknowledgement

This study was financially supported by Co-operation agreement with the Finnish concrete industry (project number 700721) and the Academy of Finland (Finnish Centre of Excellence in Inverse Modelling and Imaging, project number 336795).

References

- [1] American Concrete Institute, "Guide for Consolidation of Concrete," 2005.
- [2] P. Breul, J.-M. Geoffroy, and Y. Haddani, "On-Site Concrete Segregation Estimation Using Image Analysis," 2008.
- [3] M. Ozen and M. Guler, "Quantification of segregation in portland cement concrete based on spatial distribution of aggregate size fractions," 2020.
- [4] I. Navarrete, M. Lopez, Estimating the segregation of concrete based on mixture design and vibratory energy, *Constr. Build. Mater.* 122 (Sep. 2016) 384–390, <https://doi.org/10.1016/J.CONBUILDMAT.2016.06.066>.
- [5] P.J. M. Bartos, M. Sonebi, A.K. Tamimi, Report 24: Workability and Rheology of Fresh Concrete: Compendium of Tests – Report of RILEM Technical Committee TC 145-WSM. RILEM Publications, 2002.
- [6] M. Sonebi, *Workability and Rheology of Fresh Concrete: Compendium of Tests*. 2002.
- [7] H.A. Mesbah, A. Yahia, K.H. Khayat, Electrical conductivity method to assess static stability of self-consolidating concrete, *Cem. Concr. Res.* 41 (5) (May 2011) 451–458, <https://doi.org/10.1016/j.cemconres.2011.01.004>.
- [8] L. Shen, H.B. Jovein, M. Li, Measuring static stability and robustness of self-consolidating concrete using modified Segregation Probe, *Constr. Build. Mater.* 70 (Nov. 2014) 210–216, <https://doi.org/10.1016/j.conbuildmat.2014.07.112>.
- [9] M. Nili, M. Razmara, M. Nili, P. Razmara, Proposing new methods to appraise segregation resistance of self-consolidating concrete based on electrical resistivity, *Constr. Build. Mater.* 146 (Aug. 2017) 192–198, <https://doi.org/10.1016/J.CONBUILDMAT.2017.04.092>.
- [10] H.S. Gökçe, Ö. Andıç-Çakır, A new method for determination of dynamic stability of self-consolidating concrete: 3-Compartment sieve test, *Constr. Build. Mater.* 168 (2018) 305–312, <https://doi.org/10.1016/j.conbuildmat.2018.02.087>.
- [11] H.J. Yim, Y.H. Bae, J.H. Kim, Method for evaluating segregation in self-consolidating concrete using electrical resistivity measurements, *Constr. Build. Mater.* 232 (Jan. 2020), <https://doi.org/10.1016/j.conbuildmat.2019.117283>.
- [12] Y. Ke, A.L. Beaucour, S. Ortola, H. Dumontet, R. Cabrillac, Influence of volume fraction and characteristics of lightweight aggregates on the mechanical properties of concrete, *Constr. Build. Mater.* 23 (8) (2009) 2821–2828, <https://doi.org/10.1016/j.conbuildmat.2009.02.038>.
- [13] A.M. Solak, A.J. Tenza-Abril, F. Baeza-Brotons, D. Benavente, Proposing a new method based on image analysis to estimate the segregation index of lightweight aggregate concretes, *Materials* 12 (21) (Nov. 2019), <https://doi.org/10.3390/ma12213642>.
- [14] F.S. Barbosa, A.L. Beaucour, M.C.R. Farage, S. Ortola, Image processing applied to the analysis of segregation in lightweight aggregate concretes, *Constr. Build. Mater.* 25 (8) (Aug. 2011) 3375–3381, <https://doi.org/10.1016/j.conbuildmat.2011.03.028>.
- [15] C. Jolicoeur, K. H. Khayat, T. Pavate, and M. Pagé, "Evaluation of effect of chemical admixture and supplementary cementitious materials on stability of cement-based materials using in-situ conductivity method," *ACI Special Publication*, no. June, pp. 461–483, 2000.
- [16] K.H. Khayat, Y. Vanhove, T.V. Pavate, C. Jolicoeur, Multi-electrode conductivity method to evaluate static stability of flowable and self-consolidating concrete, *ACI Mater. J.* 104 (4) (2007) 424–433, <https://doi.org/10.14359/18833>.
- [17] K.H. Khayat, T.V. Pavate, J. Assaad, C. Jolicoeur, Analysis of Variations in Electrical Conductivity to Assess Stability of Cement-Based Materials, *ACI Mater. J.* 100 (4) (2003) pp. <https://doi.org/10.14359/12668>.
- [18] T.V. Pavate, K. Khayat, C. Jolicoeur, In-situ conductivity method for monitoring segregation, bleeding, and strength development in cement-based materials, *ACI SP 195* (Oct. 2001) 535–547.
- [19] F. Aslani, S. Nejadi, Mechanical properties of conventional and self-compacting concrete: An analytical study, *Constr. Build. Mater.* 36 (Nov. 2012) 330–347, <https://doi.org/10.1016/j.conbuildmat.2012.04.034>.
- [20] X. Hu, C. Shi, X. Liu, J. Zhang, and G. de Schutter, "A review on microstructural characterization of cement-based materials by AC impedance spectroscopy," *Cem Concr Compos.*, vol. 100, no. August 2018, pp. 1–14, 2019, doi: 10.1016/j.cemconcomp.2019.03.018.
- [21] R. Wang, F. He, C. Shi, D. Zhang, C. Chen, and L. Dai, "AC impedance spectroscopy of cement-based materials: measurement and interpretation," *Cem. Concr. Compos.*, vol. 131, no. November 2021, p. 104591, 2022, doi: 10.1016/j.cemconcomp.2022.104591.
- [22] W.J. McCarter, S. Garvin, N. Bouzid, Impedance measurements on cement paste, *J. Mater. Sci. Lett.* 7 (10) (1988) 1056–1057, <https://doi.org/10.1007/BF00720825>.
- [23] W.J. McCarter, G. Starrs, T.M. Chrisp, The complex impedance response of fly-ash cements revisited, *Cem. Concr. Res.* 34 (10) (Oct. 2004) 1837–1843, <https://doi.org/10.1016/J.CEMCONRES.2004.01.013>.
- [24] J. Jain, N. Neithalath, Electrical impedance analysis based quantification of microstructural changes in concretes due to non-steady state chloride migration, *Mater. Chem. Phys.* 129 (1–2) (2011) 569–579, <https://doi.org/10.1016/j.matchemphys.2011.04.057>.
- [25] W.J. McCarter, H.M. Taha, B. Suryanto, G. Starrs, Two-point concrete resistivity measurements: Interfacial phenomena at the electrode-concrete contact zone, *Meas. Sci. Technol.* 26 (8) (2015) pp. <https://doi.org/10.1088/0957-0233/26/8/085007>.
- [26] W.J. McCarter, G. Starrs, T.M. Chrisp, Immittance spectra for Portland cement/fly ash-based binders during early hydration, *Cem. Concr. Res.* 29 (3) (Mar. 1999) 377–387, [https://doi.org/10.1016/S0008-8846\(98\)00209-9](https://doi.org/10.1016/S0008-8846(98)00209-9).
- [27] A. Princigallo, K. Van Breugel, G. Levita, Influence of the aggregate on the electrical conductivity of Portland cement concretes, *Cem. Concr. Res.* 33 (11) (Nov. 2003) 1755–1763, [https://doi.org/10.1016/S0008-8846\(03\)00166-2](https://doi.org/10.1016/S0008-8846(03)00166-2).
- [28] T.C. Hou, V.K. Nguyen, Y.M. Su, Y.R. Chen, P.J. Chen, Effects of coarse aggregates on the electrical resistivity of Portland cement concrete, *Constr. Build. Mater.* 133 (Feb. 2017) 397–408, <https://doi.org/10.1016/j.conbuildmat.2016.12.044>.
- [29] W.J. McCarter, A parametric study of the impedance characteristics of cement-aggregate systems during early hydration, *Cem. Concr. Res.* 24 (6) (Jan. 1994) 1097–1110, [https://doi.org/10.1016/0008-8846\(94\)90034-5](https://doi.org/10.1016/0008-8846(94)90034-5).

- [30] W.J. McCarter, The a.c. impedance response of concrete during early hydration, *J. Mater. Sci.* 31 (23) (1996) 6285–6292, <https://doi.org/10.1007/BF00354451>.
- [31] J. Park, D. Kim, S. Shim, J. Hong, H. Choi, S.S. Jin, Water-cement ratio estimation of cementitious materials using electrochemical impedance spectroscopy and machine learning, *J. Korea Concr. Inst.* 33 (4) (2021) 353–361, <https://doi.org/10.4334/JKCI.2021.33.4.353>.
- [32] Y. Zhu, H. Zhang, Z. Zhang, Y. Yao, Electrochemical impedance spectroscopy (EIS) of hydration process and drying shrinkage for cement paste with W/C of 0.25 affected by high range water reducer, *Constr. Build. Mater.* 131 (2017) 536–541, <https://doi.org/10.1016/j.conbuildmat.2016.08.099>.